Journal of Computers Vol. 30 No. 6, 2019, pp. 263-275
doi:10.3966/199115992019123006022

Aesthetic QR Code Authentication Based on Directed Periodic Texture Pattern

Li Li[1], Min He[1], Jier Yu[1], Jianfeng Lu[1*], Qili Zhou[1], Xiaoqing Feng[2], Chin-Chen Chang[3]

[1] Department of Computer Science, Hangzhou Dianzi University, Hangzhou 407, Zhejiang, China
{lili2008, jflu,zql}@hdu.edu.cn, HMin0919@outlook.com, 2271092014@qq.com

[2] Department of Computer Science, Zhejiang University of Finance and Economics,
Hangzhou 407, Zhejiang, China
fenglinda@zufe.edu.cn

[3] Department of Information Engineering and Computer Science, Feng Chia University,
Taichung 403, Taiwan
alan3c@gamil.com

Received 10 May 2019; Revised 10 June 2019; Accepted 2 July 2019

Abstract. More and more people use mobile phones to buy goods through scanning the printed aesthetic QR code. QR code has become an important payment tool in to-day's business. However, there is an inevitable risk in payment processing. In particular, it is difficult to detect whether an aesthetic QR code has been tampered by the attacker. Therefore, it is extremely important to carry out security certification for aesthetic QR code. We propose an algorithm based on the combination of directional periodic texture pattern and aesthetic QR code. Firstly, the aesthetic QR code is generated based on the Positive Basis Vector Matrix (PBVM), whereas the watermark is encoded into 4-bit Gray code and quantized into angles. Then, a periodic texture pattern is generated using a random matrix, and a directed periodic texture pattern is obtained by rotating the texture pattern according to the quantization angle. Finally, the new texture pattern and the aesthetic QR code are fused to obtain an authentication aesthetic QR code. The experiments verified that the aesthetic QR code can be correctly decoded and the watermark can be properly extracted. By utilizing the locating position patterns of the QR code, the additional watermark reference block is not required, therefore, the capacity of the watermark is enhanced. Moreover, the proposed scheme realizes the anti-counterfeiting authentication of aesthetic QR code, and maintains a better visual quality.

Keywords: aesthetic QR Code, authentication, watermark

1 Introduction

With the rapid development of the Internet, mobile phones are replacing personal computers due to their small size and portability. Mobile phones can capture, store and share images more quickly. In the marketplace, many applications are accompanied with QR code scanning, for example, website jumps, payment, and sales promotion. QR code stores a large amount of data and yet is independent of the database. It also has strong error correction capability. Furthermore, it can be decoded anywhere by using a smart phone. Therefore, it is widely used in some security sensitive applications, such as mobile payments [1-2].

* Corresponding Author

Since there is no anti-counterfeiting function in traditional QR code, the attacker can easily tamper with a QR code. More and more researchers worked on improving the visual effects of the traditional QR code. As a result, various algorithms of aesthetic QR cod were proposed [3-4]. At the same time, for enhancing the security certification of aesthetic QR code, some security authentication methods for aesthetic QR code were presented. For example, Lu et al. [5] proposed an algorithm based on visual cryptography scheme (VCS) combined with aesthetic QR code, which utilizes the visual cryptography divides an original QR code into two shadows, then two shadows are separately embedded into the same background image, and uses the XOR operation to fuse the embedding results with the same carrier QR code. This method can correctly verify the security of the QR code in the mobile payment process. Li et al. [6] presented a multi-safety authentication for aesthetic QR code for shared bicycles, it combines aesthetic QR code with color visual passwords. Two methods in above have good visual quality, but are fragile to print attack.

Print-cam [7] is the process of printing an image and then taking it photos using a mobile phone. During this process, there are some common attacks such as distortion, rotation, scaling, translation, and cropping. In addition, depending on the accuracies of printers, different types of noises will be imposed to the image. These distortions increase the difficulty of extracting the watermark.

However, not many schemes were proposed to protect watermark against print-cam. Katayama et al. [8] firstly proposed a print-cam robust watermark that is based on a sinusoidal watermark pattern and frame synchronization. This method needs to use watermark template positioning, which increases the complexity of watermark extraction. Then, Kim et al. [9] presented watermark extraction using autocorrelation function. They embed pseudo-random vectors by repeating tiling, and then detect the resulting peaks by autocorrelation functions. The method was tested on a digital camera. However, manual interaction must be applied during extracting the water-mark. In order to improve the robustness of the watermark in the print-cam process, Pramila et al. [10] modified Chou's methods [11] using autocorrelation functions and directed periodic patterns. The patterns rotated at the angle generated by the water-mark message encoding. This method is robust against ±10° of the tilt of the optical axis, but the embedding capacity is low. At the same time, the method combines the spatial masking and the background luminance components in the JND (just notice-able difference) model. Instead of selecting only one of them, they took more image details into account and made the image look better.

Inspired by directed periodic patterns [10], the watermark is embedded into the aesthetic QR code based on the positive basis vector matrix using the directional periodic texture pattern. During detecting the watermark, the position patterns of the aesthetic QR code are utilized, and no additional watermark reference block is need-ed. As a result, this scheme not only improves the capacity of watermark, but is also robust against print attack. Moreover, it realizes the QR code anti-counterfeiting authentication.

The rest of this paper is organized as follows. Aesthetic QR code generation and watermark embedding are introduced in Section 2. In Section 3, the extraction and detection watermark are described in detailed. In Section 4, we show the experimental results. Finally, conclusion and future work are given in Section 5.

2 Watermark Embedding

In Section 2, the watermark embedding process is described in detail. Firstly, an aesthetic QR code is generated based on the PBVM. Then, the aesthetic QR code is pre-processed and the JND value is computed. In order to maintain visual quality, the embedding strength is controlled by JND. Secondly, the watermark message is encoded using Hamming (32, 6) error correction coding and 4-bit Gray coding. Each Gray code sequence is converted to a rotation angle. The periodic texture pattern is rotated according to the angle in order to get a new texture pattern. Finally, the JND and new texture pattern is fused with the aesthetic QR code. The overview of the watermark embedding process is shown in Fig. 1.

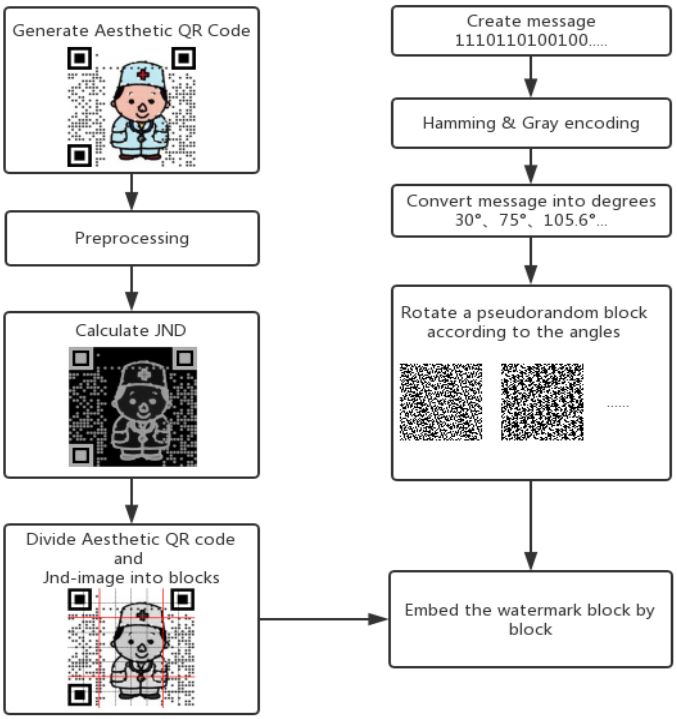

Fig. 1. The embedding process

2.1 The Generating Algorithm of Aesthetic QR Code

Image preprocessing. To increase the decoding rate of the QR code, image preprocessing methods are applied on the input background image. The flowchart is shown in Fig. 2.

Fig. 2. The flowchart of image preprocess

Firstly, the background image I_0 is converted from RGB color space to Lab color space. Then the image's brightness channel is stretched to improve the contrast. In the new image I_1, the pixels are stretched to both sides according to the corresponding ratio. The pre-processed image is converted into gray scale image I_2 and compressed to the same size as the original QR code image for subsequent operations.

Construction of QR code based on PBVM. A series of RS codes obtained by Gauss Jordan elimination method formulates a matrix. The matrix is called Positive Basis Vector Matrix (PBVM). When a bit of RS code needs to be modified, special row in the PBVM is selected to execute XOR operation so that the bit is flipped. Based on this principle, we can construction a basic QR code image which is similar to the background image.

The fusion strategy. The basic QR code image constructed by the PBVM are fused with preprocessed the background image to get the final aesthetic QR code.

The fusion strategy used in this paper is referenced from literature [12]. In the Eq. (1), T_i represents gray average of gray block. T_0 represents binary threshold, which is obtained from Otsu's method. N_i is the module of QR code, $N_i = 1$ represents white block and $N_i = 0$ represents black block. Where Q=0 represents that the background image is completely replaced; Q = −1 or 1 represents the central region of

the specified module is replaced by the corresponding region of the QR code, and the other region is replaced by corresponding region of background image. Finally, aesthetic QR code is obtained.

$$Q=\begin{cases} 0, & T_i < T_0 \bigcap N_i = 0, \\ -1, & T_i > T_0 \bigcap N_i = 0, \\ 1, & T_i < T_0 \bigcap N_i = 1, \\ 0, & T_i > T_0 \bigcap N_i = 1. \end{cases} \tag{1}$$

2.2 The Fusion of Aesthetic QR Code and Texture Pattern

Step 1: Pretreatment for aesthetic QR code. Aesthetic QR code I is changed from the RGB color space to YUV color space, and the Y-channel is preprocessed using the Wiener filter, denoted as I_w. The Wiener filter minimizes the mean square error between the aesthetic QR code I and the filtered QR code I_w. It is an adaptive filter and has a significant effect on removing Gaussian noise. In order to break the periodicity in the aesthetic QR code I, a part of Wiener filter is replaced with the original image, and the I_p is generated. The replace method is shown in Eq. (2).

$$I_p(x,y)=\begin{cases} I_w(x,y), \textit{when } r(x,y)=1 \textit{ and } (I(x,y)-I_{w(x,y)}>0), \\ I(x,y) \qquad\qquad \textit{otherwise.} \end{cases} \tag{2}$$

where r is random matrix with the same size as the aesthetic QR code and contains only 0 and 1, the sum of the probabilities of 0 and 1 is 1. By controlling the probability of 1 in the matrix, more image details are available to maintain visual quality.

Step 2: Calculated the JND value. To ensure the robustness of the print-cam process, calculating the JND value of the aesthetic QR code I_p to measure the sensitivity of people to different areas of distortion. In paper [11], the JND is calculated as follows:

$$JND(x,y)=\lambda_1\times(f_1(bg(x,y),mg(x,y))+\lambda_2)+f_2(bg(x,y), \tag{3}$$

$$f_1(bg(x,y),mg(x,y))=bg(x,y)\times\alpha(bg(x,y))+\beta(bg(x,y)), \tag{4}$$

$$f_2(bg(x,y))=\begin{cases} T_0\times(1-\sqrt{(\frac{bg(x,y)}{127})})+3, & for\ bg(x,y)\le 127, \\ \gamma\times(bg(x,y)-127)+3, & for\ bg(x,y)>127, \end{cases} \tag{5}$$

$$\alpha(bg(x,y)=bg(x,y)\times 0.0001+0.115), \tag{6}$$

$$\beta(bg(x,y)=\lambda-bg(x,y)\times 0.1 \tag{7}$$

where f_1 represents the spatial masking component, $bg(x,y)$ is the average background luminance, $mg(x,y)$ represents the maximum weighted average of luminance differences. $\alpha(x,y)$ is the slope of the f_1, $\beta(x,y)$ represents the intersection with the visibility threshold axis. f_2 is the visibility threshold. The value of T_0, γ and λ to be 17, 3/128 and 1/2. λ_1 and λ_2 are scaling factors. The values are λ_1=2.0 and λ_2=3.0.

Step 3: Transform watermark message into angle. The watermark is embedded in the aesthetic QR code by dividing the QR code into blocks. The capacity of embedded is the total bits of all blocks. In our experiments, the aesthetic QR code is divided into non-overlapping 8×8 blocks, each block are 64×64 pixels. In order to guarantee the decoding rate of the aesthetic QR code, the non-data area of the QR code is used. A center size of 256×256 pixels of QR code I_p is divided into 4×4 blocks, which is expressed as I_k (k =1…16). 4 bits are embedded in each block and the capacity of watermark is 64 bits. The JND

image is divided into block according to the QR code block, denoted as J_k (k1…16). The block diagram is shown in Fig. 3.

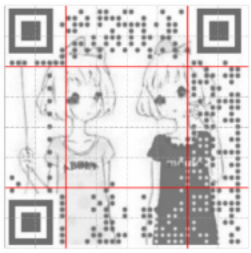

Fig. 3. The flowchart of image preprocess

The watermark message S= $\{S_1, S_2, \ldots, S_n\}$ is encoded using Hamming (32, 6) error correction coding and 4-bit Gray coding. Firstly, Hamming (32, 6) codes can detect up to two-bit errors. 4 bits per block is divided according to the errors sequence. Secondly, each 4 bits is encoded into 4-bit Gray coding. Each Gray code sequence is converted to a rotation angle, which is assigned a value between 0 and 180 degrees. The angle is quantified according to the number of embedded bits, and then allocated to each Gray coded sequence. If each block is embedded with 4 bits, the quantization angle is given in Table 1. The quantization step size of the angle is calculated by the Eq. (8).

Table 1. Quantizing the rotation angles

Gray code	Quantization angle
0000	0°-11.25°
0001	11.25°-22.5°
0011	22.5°-33.75°
0010	33.75°-45°
0110	45°-56.25°
0111	56.25°-67.5°
0101	67.5°-78.75°

$$\alpha = \frac{180°}{2^m}. \tag{8}$$

where m represents the bits embedded in per block.

Because the adjacent quantization step size of the Gray code is only 1 bit, when the rotation angle of the texture is misinterpreted, the Hamming code and the Gray code can ensure that the watermark message is correctly extracted.

Step 4: Generate the texture patterns. The texture pattern rotates according to the encoded message. Texture patterns W is generated by tiling a small pseudo-random matrix, the pseudo-random pattern $w(x, y)$ ($1 \le$ x ≤ 28, $1 \le$ y ≤ 7) is a random matrix containing only {−1, 1} of size 28×7.

The periodicity of texture pattern W is shown in Eqs. (9) and (10).

$$W(x + hp_0, y) = w(x, y); h, p_0 > 1, \tag{9}$$

$$W(x, y + vp_1) = w(x, y); v, p_1 > 1. \tag{10}$$

where p_0 and p_1 represent the number of repetitions of the periodicity, h and v denote the number of repetitions in both horizontal and vertical directions.

The texture pattern W is 128×128 pixels. Each texture is rotated in turn by the angle and cut the size to 64×64.

A directed periodic texture pattern is calculated by the Eq. (11).

$$W^{\theta} = W(u', v') + \varepsilon = \Pi\left\{\begin{bmatrix} \cos\theta & -\sin\theta \\ \sin\theta & \cos\theta \end{bmatrix} \times W(u, v)\right\}. \tag{11}$$

where Π defines bilinear interpolation and ε represents the error. θ defines the rotation angle.

Step 5: *The fusion of watermark.* The JND image block J_k and directed periodic texture pattern block $W_k^{\theta_k}$ are fused with aesthetic QR code blocks $I_k(k = 1...16)$. The watermark fusion algorithm is shown in Eq. (12).

$$I_k'(x, y) = I_k(x, y) + W_k^{\theta_k}(x, y)(\delta_1 J_k(x, y) + \delta_2(1 - J_k(x, y))). \tag{12}$$

where I_k' is the kth watermark block of the aesthetic QR code, the parameters δ_1 and δ_2 determine the embedded strength. The watermark strength of δ_1=40, δ_2=4 and δ_1=50, δ_2=5 are demonstrated in Fig. 4.

(a) Original image (b) δ_1=40, δ_2=4 (c) δ_1=50, δ_2=5

Fig. 4.

3 Watermark Extraction and Message Detection

Fig. 5 shows the flow of the watermark extraction process. An aesthetic QR code captured by mobile phone and the captured image is corrected using QR code positioning information. The Y-channel of the captured image is preprocessed and then divided into blocks. These blocks are processed by calculating the autocorrelation function of each block and enhancing the autocorrelation peak. Then, lines are searched from the autocorrelation image using Hough Transform in order to obtain angles. Finally, the watermark is decoded by the angles using Gray and Hamming codes

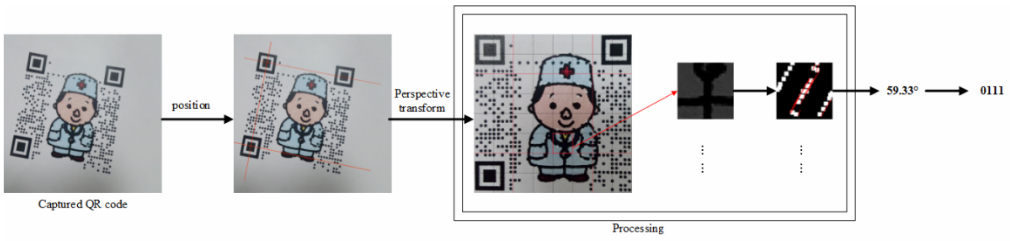

Fig. 5. The flowchart of image preprocess

3.1 Correction of QR Code

In the print-cam process, the common distortion are rotation, scaling, translation, and cropping. In order to extract message, the aesthetic QR code Y_q captured by the mobile phone should be projected to a new viewing plane by perspective transformation. Firstly, the three position patterns of QR code rapidly locate the center point coordinates. Then, the four control points of the target image calculated by the four vertex coordinates. Finally, geometric distortion correction is accomplished by perspective

transformation. The corrected image is denoted as Y_p. The positioned and corrected image are illustrated in Fig. 6.

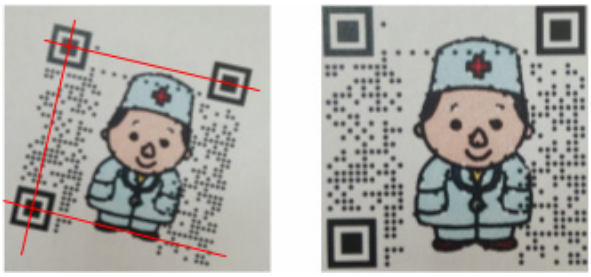

Fig. 6. QR Code positioning and correction

In addition, the image Y_p is down-sampled by using bilinear interpolation, denoted as Y_p'. Then, the image Y^* is obtained by adjusting the brightness and contrast.

3.2 Calculation of Autocorrelation Function

The center size of the 256×256 of the image Y^* is chosen, and then divided into 4×4 blocks, which is expressed as $Y_k^*(k=1...16)$. For each block, the median filter removes outliers and noise from the image is to be calculated by the Eq. (13).

$$\widetilde{W}_k(x,y) = Y_k^*(x,y) - h_m(k) * Y_k^*(x,y). \tag{13}$$

where $Y_k^*(x,y)$ is the kth watermarked block and h_m represents the median filtering.

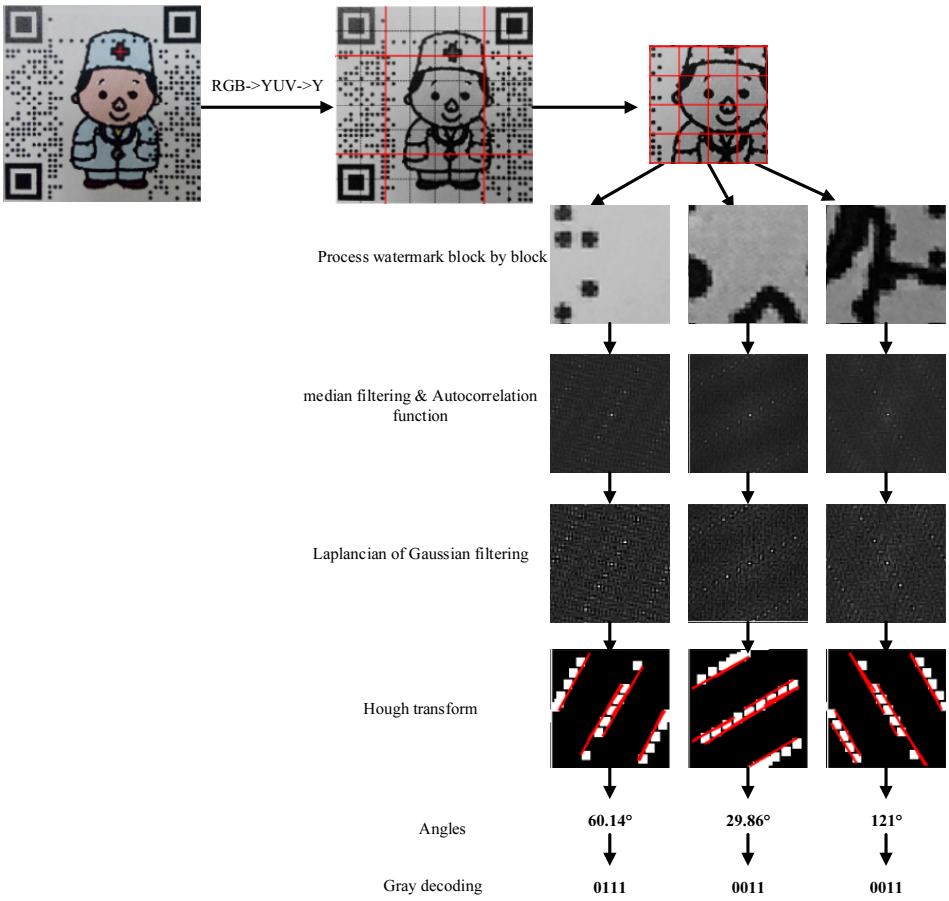

Fig. 7. The message extraction

Autocorrelation function is a common method for spatial frequency texture description. The periodicity of autocorrelation function reflects the periodicity of repeated occurrence of texture primitives. The autocorrelation function of regular texture has peaks and valleys, which can be used to detect the arrangement of texture elements. The median filtered image $\widetilde{W}_k$ calculates the autocorrelation function to get Y_R^*. The autocorrelation function is shown in Eq. (14).

$$R_{\widetilde{W}_k\widetilde{W}_k}(u,v)=\sum_x\sum_y\widetilde{W}_k(x,y)\widetilde{W}_k(x+u,y+v). \tag{14}$$

The resulting values of the autocorrelation is normalized between 0 and 1.

$$R^*_{\widetilde{W}_k\widetilde{W}_k}(u,v)=\frac{|R_{\widetilde{W}_k\widetilde{W}_k}(u,v)|}{\max(R_{\widetilde{W}_k\widetilde{W}_k}(u,v))}. \tag{15}$$

In order to enhance the peak detection of autocorrelation function, rotationally symmetric Laplacian of Gaussian filtering operation is performed in Eq. (16).

$$R^{**}_{\widetilde{W}_k\widetilde{W}_k}(u,v)=\frac{\partial^2}{\partial(u,v)^2}h^T*(\frac{\partial^2}{\partial(u,v)^2}h\times R^*_{\widetilde{W}_k\widetilde{W}_k}(u,v)). \tag{16}$$

The morphological operation usually uses a structuring element for probing and expanding the shapes containing in the input image. A structuring element $G(u,v)$ is generated by the Eq. (17).

$$G(u,v)=\begin{cases}1,\ if\ M(u,v)\times R^{**}_{\widetilde{W}_k\widetilde{W}_k}(u,v)\geq\gamma,\\ 0,\ if\ M(u,v)\times R^{**}_{\widetilde{W}_k\widetilde{W}_k}(u,v)<\gamma.\end{cases} \tag{17}$$

where $M(u,v)$ denotes masking operation and γ is a threshold. Threshold operation is used to find the location of the maximum value in the autocorrelation function. γ is mainly used to control sufficient peaks for line detection.

3.3 Watermark Message Extraction

Lines are detected from the structuring element using Hough Transform. Each quantified angle represents each block of watermark message, as show in Table 1. Finally, the watermark message is decoded by Hamming (32, 6) code. Then, the message of all the blocks is connected to obtain the watermark. The flow chart of message detection is illustrated in Fig. 7.

4 Experiments

4.1 Subjective Evaluation

The system was implemented by MATLAB. In the experiments, all the test images are of size 512×512 and each aesthetic QR code is embedded with different watermarks. We utilized HP Color LaserJet 1025 PCL 6 printer. The physical size of the printed images is 6×6 cm. The watermark images are printed on A4 paper, and all experiments are carried out in a normal indoor lighting environment. Part of the test images, watermark images and the print-cam images are given in Table 2.

Table 2. The test images

Test images	Watermark images (δ_1 =40, δ_2 =4)	Print-cam images
		
		
		
		
		
		

The quality of the watermark images are evaluated by subjective testing. The strengths of watermark images are δ_1 =40, δ_2 =4 and δ_1 =50, δ_2 =5. Ten persons are invited to evaluate the original images and watermarked ones. The five-point scale is rated on images: (5: imperceptible, 4: perceptible but not objectionable, 3: slightly objectionable, 2: objectionable, 1: very objectionable). The results of subjective evaluation are shown in Table 3.

Table 3. Subjective evaluation scores of watermark images

Strength	δ_1 =40, δ_2 =4	δ_1 =50, δ_2 =5
image1	4.81	4.66
image2	4.85	4.78
image3	4.84	4.67
image4	4.78	3.93
image5	4.97	4.75
image6	4.95	4.58

4.2 Objective Evaluation

For image quality analysis, objective evaluation has measured by SSIM (structural similarity index) [13]. Given two aesthetic QR codes x and y, the structural similarity of the two images can be found as follows:

$$SSIM(x, y) = \frac{(2u_x u_y + c_1)(2\sigma_{xy} + c_2)}{(u_x^2 + u_y^2 + c_1)(\sigma_x^2 + \sigma_y^2 + c_2)}. \quad \textbf{(18)}$$

where u_x the average of x, u_y the average of y, σ_x^2 the variance of x, σ_y^2 the variance of y, σ_{xy} the covariance of x and y, $c_1 = (k_1 L)^2$, $c_2 = (k_2 L)^2$ two variables to stabilize the division with weak denominator. L the dynamic range of the pixel-values, k_1 =0.01, k_2 =0.03 by default.

The value of SSIM is between -1 and 1, where value 1 indicates that two images are the same. The experiment result shows our algorithm has good visual quality when the watermark strength is lower than δ_1 =70, δ_2 =7, while the SSIM is greater than 0.8. The obtained results are shown in Table 4.

Table 4. Image quality by SSIM

Strength	δ_1 =40, δ_2 =4	δ_1 =50, δ_2 =5	δ_1 =60, δ_2 =6	δ_1 =70, δ_2 =7
image1	0.9311	0.9122	0.9010	0.8882
image2	0.9724	0.9641	0.9554	0.9477
image3	0.9623	0.9438	0.9230	0.9105
image4	0.9206	0.9020	0.8879	0.8814
image5	0.9747	0.9677	0.9631	0.9576
image6	0.9785	0.9720	0.9624	0.9543

4.3 Robustness against Distance Variations

To make sure the aesthetic QR code decoded correctly, the range of the mobile phone from A4 paper is constantly changed. These experiments are tested with Xiaomi 8 mobile phone, a 1200 megapixel CMOS camera. Wide-angle lens is 28 mm and aperture F1.8. Test images are printed on an A4 paper, using HP Color LaserJet 1025 PCL 6 printer.

Fig. 8 shows the captured image using mobile phone. The captured image is segmented into blocks and the average precision of the rotation angle of each block is calculated. The accuracy of angle detection is determined by the relative error between the calculated average angle and the actual angle. The smaller the error, the higher the accuracy of the test results. In the experiment, the watermark is correctly extracted at a watermark strength of δ_1 =50, δ_2 =5 and a distance between 8 and 18. The experimental results are illustrated in Fig. 9.

Fig. 8. Examples of captured images at different distances

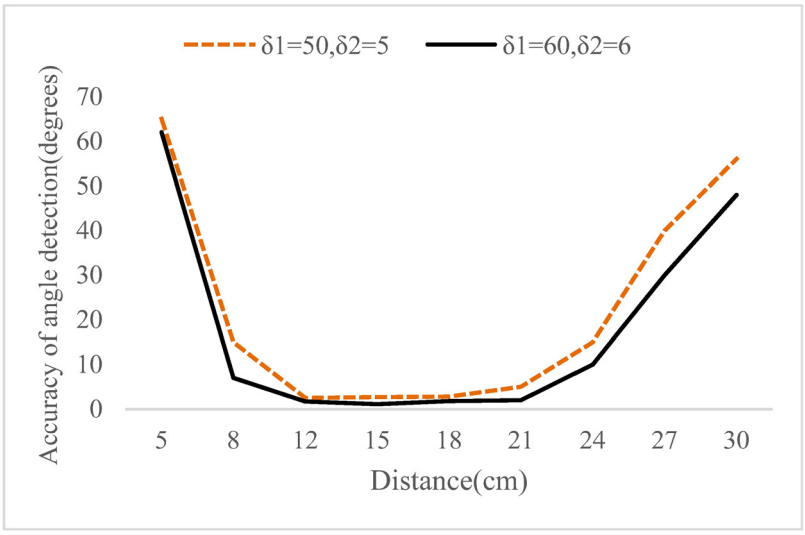

Fig. 9. Effect of distance on angle accuracy

4.4 Robustness against Angle Variations

For testing robustness at various angles, different angles of the test image are taken at the same distance, and the watermark bits extracted correctly is calculated. The captured images at various angles are shown in Fig. 10. If each block is embedded with 4 bits, the correct extraction result of the watermark is given in Table 5 when the strength is δ_1 =50, δ_2 =5. Table 6 shows the experimental results generated by embedding 5 bits into each block. Compared with [10], our algorithm utilizing the locating position patterns of the QR code, the additional watermark reference block is not required. The proposed algorithm not only improves the embedding capacity of the watermark, but also increases the angle range of the captured image.

Fig. 10. Examples of captured images at different angles

Table 5. Robustness to attacks with 64bit message (Sixteen 4 bit message segments embedded)

Angle	0°	5°	10°	15°	20°	25°
image1	64/64	64/64	64/64	64/64	63/64	62/64
image2	64/64	64/64	64/64	63/64	62/64	61/64
image3	64/64	64/64	64/64	64/64	64/64	63/64
image4	64/64	64/64	64/64	64/64	63/64	62/64
image5	64/64	64/64	64/64	61/64	60/64	59/64
image6	64/64	64/64	64/64	64/64	64/64	63/64

Table 6. Robustness to attacks with 80 bit message (Sixteen 5 bit message segments embedded)

Angle	0°	5°	10°	15°	20°	25°
image1	80/80	80/80	80/80	75/80	78/80	76/80
image2	80/80	80/80	80/80	77/80	79/80	75/80
image3	80/80	80/80	80/80	78/80	80/80	79/80
image4	80/80	80/80	80/80	80/80	79/80	80/80
image5	80/80	80/80	80/80	76/80	78/80	79/80
image6	80/80	80/80	80/80	80/80	79/80	78/80

The test results show that when the aesthetic QR code is taken vertically, the watermark strength of δ_1=50, δ_2=5 is sufficient to extract the watermark correctly from all the images. When each block is embedded with 4 bits, the quantization range of the angle is larger than 5 bits per block. It is shown that embedding more bits into each block will reduce the degree of quantification, and therefore the robustness of the watermark is reduced. The angle of shooting for all printed images is robust to 15 degree tilt when 4 bits are embedded each block.

5 Conclusion

A novel authentication algorithm for aesthetic QR code based on positive basis vector matrix and directed texture pattern is proposed. This method realizes dual security authentications of aesthetic QR code and maintains a better visual quality. By utilizing the locating position patterns of the QR code, the additional watermark reference block is not required. Moreover, the proposed scheme not only enhances the watermark capacity, but also improves the watermark robustness against the print-cam process.

In the future, we hope to improve the robustness and imperceptibility of the watermark. The unused QR code region during the embedding process deserves further investigations.

Acknowledgements

This work was mainly supported by National Natural Science Foundation of China (No. 61370218, No. GG19F020033), Public Welfare Technology and Industry Project of Zhejiang Provincial Science Technology Department (No. 2016C31081, No. LGG18F020013, No. LGG19F020016).

References

[1] H. Suryotrisongko, Sugiharsono, B. Setiawan, A novel mobile payment scheme based on secure quick response payment with minimal infrastructure for cooperative enterprise in developing countries, Procedia- Social and Behavioral Sciences 65(3)(2012) 906-912.

[2] D.A. Ortiz-Yepes, A review of technical approaches to realizing near-field communication mobile payments, IEEE Security & Privacy 14(4)(2016) 54-62.

[3] Q. Ahmed, S. Munib, M.T. Mirza, A. Khan, Smart phone based online medicine authentication using print-cam robust watermarking, in: Proc. 2015 13th International Conference on Frontiers of Information Technology, 2015.

[4] M. Kuribayashi, M. Morii, Aesthetic QR code based on modified systematic encoding function, IEICE Transactions on Information and Systems 1(E100D) (2017) 42-51.

[5] J.F. Lu, Z.R. Yang, L. Lina, W.Q. Yuan, L. Li, C.C. Chang, Multiple schemes for mobile payment authentication using QR code and visual cryptography, Mobile Information Systems 9(2017) 1-12.

[6] L. Li, L. Lina, S.Q. Zhang, Z.R. Yang, J.F. Lu, C.C. Chang, Novel schemes for bike-share service authentication using aesthetic QR code and color visual cryptography, in: Proc. International Conference on Cloud Computing and Security Third International Conference, 2017.

[7] A. Pramila, A. Keskinarkaus, T. Seppänen, Increasing the capturing angle in print-cam robust watermarking, Journal of Systems and Software 135(2018) 205-215.

[8] A. Katayama, T. Nakamura, M. Yamamuro, N. Sonehara, New highspeed frame detection method: side trace algorithm (STA) for i-appli on cellular phones to detect watermarks, in: Proc. the 3rd International Conference on Mobile and Ubiquitous Multimedia, 2004.

[9] W. Kim, H.J. Jang, G.Y. Kim, Transmission rate prediction of VBR motion image using the kalman filter, in: Proc. International Conference on Computational Science and Its Applications, 2006.

[10] A. Pramila, A. Keskinarkaus, T. Seppänen, Toward an interactive poster using digital watermarking and a mobile phone camera, Signal Image and Video Processing 6(2)(2016) 211-222.

[11] D.H. Chou, Y.C. Li, A perceptually tuned subband image coder based on the measure of just-noticeable-distortion profile, IEEE Transactions on Circuits and Systems for Video Technology 5(6)(1995) 467-476.

[12] L. Li, W. Bing, J.F. Lu, S.Q. Zhang, C.C. Chang, A New Aesthetic QR Code Algorithm Based on Salient Region Detection and SPBVM, Journal of Internet Technology 3(20)(2019) 935-946.

[13] A. Hore, D. Ziou, Image quality metrics: PSNR vs. SSIM, in: Proc. 2010 20th International Conference on Pattern Recognition, 2010.